Power-to-heat plants in district heating and electricity distribution systems: A techno-economic analysis

Power-to-Heat plants in district heating and electricity distribution systems: a techno-economic analysis

Gabriele Fambri, Andrea Mazza, Elisa Guelpa, Vittorio Verda, Marco Badami

Dipartimento Energia, Politecnico di Torino, Corso Duca degli Abruzzi 24, 10129 Torino, Italy

HIGHLIGHTS

- The flexibility of district heating-connected heat pumps was investigated
- The utilization of heat pump could help to electrify the district heating sector
- Heat pump technology resulted a viable solution to provide heat in district heating
- The heat pump flexibility could improve the electricity distribution system balance
- Exploiting the heat pump flexibility strongly increases the heat pump profitability

ABSTRACT

This paper investigates the Power-to-Heat energy conversion process carried out by heat pumps connected to a District Heating network used to pro Heating ide heat to the heating sector and, at the same time, to provide flexibility for the electricity sector. The aim of this work is to analyze from a techno-economic point of view the flexibility potential of this solution used to absorb the over-generation of Variable Renewable Energy Sources in the distribution system. A scenario, based on the electric distribution system and the District Heating distribution system of the city of Turin, was created to carry out this type of study. The results showed that, flexible use of these Power-to-Heat systems can be exploited to shift part of electric loads in periods of renewable over-generation, with significant benefits from an economic point of view. Furthermore, the position of Power-to-Heat systems within an electricity distribution network has a significant impact; to make the most out of the flexibility of these plants, they should be placed in those areas of the network that present the greatest local over-generation of renewables. The use of heat pumps will be necessary for the energy transition thanks to the high conversion efficiency. However, in order to fully exploit all the benefit that this technology can offer its flexibility cannot be ignored.

KEYWORDS

Renewable energy integration, District heating system, Electricity distribution system, Multi energy system, Power-to-Heat, techno-economic analysis.

ACRONYMS

BFS	Backward Forward Sweep
CAPEX	Capital Expenditure
CHP	Combined Heat and Power
CO_2	Carbon dioxide
COP	Coefficient of Performance
DH	District Heating
EER	Energy Efficiency Ratio
EN	Electricity Network
DSO	Distribution System Operator
HP	Heat Pump
HV	High Voltage
MES	Multi-Energy System
NPV	Net Present Value
O&M	Operation and Maintenance
MV	Medium Voltage
P2G	Power-to-Gas
P2H	Power-to-Heat
P2X	Power-to-X
RPF	Reverse Power Flow
SN	DH Sub-Network
SoC	State of Charge
SPB	Simple Pay Back
PV	Photovoltaic plants

TES	Thermal Energy Storage
TR	Transformer
TSO	Transmission System Operator
RES	Variable Renewable Energy Sources

1. Introduction

The most recent climate data have shown that, in the last decade, the global average temperature has been 1.09°C higher than the levels of the late nineteenth century [1]. Scientific evidence shows that this trend is closely related to the increase in anthropogenic carbon dioxide emissions [2]. The European Union, with the Clean Energy for all Europeans legislation package [3], aims to reach carbon neutrality by 2050. In this context, Variable Renewable Energy Sources (VRES) will play a fundamental role in decarbonizing the entire energy system. However, VRES (wind and solar sources) are, by nature, non-dispatchable, highly volatile and intermittent, and this makes a balance between energy generation and demand difficult [4]. In fact, the electricity distribution system has not been designed to manage bi-directional power flows. During the inevitable periods of uncontrolled renewable energy over-generation, the energy produced by the distributed resources connected to the distribution system is fed into the transmission system. This phenomenon, which is called Reverse Power Flow (RPF), should be avoided, as it is not possible to maintain the proper operation of the distribution system under these conditions [5]. When RPF occurs, the current solution is to cut off the production of VRES. This, in addition to being a cost in terms of energy efficiency, is also an economic cost. For example, in 2016, a total of 373 Million Euros was spent in Germany to compensate for the operators of VRES plants for 3.7 TWh of the curtailed electricity [6]. In order to exploit VRES, it is necessary to adopt solutions and technologies that allow the energy balance to be modulated [7]; this characteristic is referred to as flexibility, and it can be defined as "*the capability of a system to modify its energy generation/consumption profile in order to offer ancillary services to the grid*" [8]. Energy storage technologies, such as electric batteries [9], pumped hydro storage [10] and compressed-air energy storage [11], can offer the required flexibility, although this kind of solution is normally penalized by high investment costs. New and cheaper sources of flexibility can arise, thanks to the coupling of other energy sectors [12]: a holistic approach that not only considers the electricity sector according to the principle of the Multi-Energy System (MES) approach allows the synergies between the different energy-intensive sectors to be exploited [13]. In fact, it is known that storing energy in non-electrical form (for example in the form of heat) is much easier and cheaper than storing electrical energy [14]. Moreover, the non-electricity energy sectors do not require a constant balance between generation and energy consumption, and this intrinsic characteristic of flexibility can be transferred to the electricity sector, thanks to Power-to-X (P2X) energy conversion technologies [15]. Various flexible solutions that emerge from the coupling of different energy sectors have been analyzed in the literature, such as electric mobility [16], the gas sector [17] and hydrogen-based applications [18]. This article analyzes the flexibility that can be derived from the coupling of the electricity distribution system with the district heating. The two energy infrastructures are connected through the use of centralized Heat Pumps (HP), which convert electricity into heat. In literature, these technologies are called Power-to-Heat (P2H) and they include other types of technologies, such as electric boilers [19]. This article focuses only on HP, and the term P2H will be used henceforth to refer to HP systems.

1.1. Power-to-Heat in district heat networks

P2H systems are used in DH to increase the water temperature to a maximum temperature of about 100°C [20], although the latest technological advances have shown potentials of up to 160°C [21]. Their thermal power ranges between some kW to more than 10 MW. Air [22], groundwater [23], river/lake/seawater [24], drinking water [25] and waste heat [26] are among the sources that can be used to feed heat pumps in DH networks. In 2017, the analysis reported in [27] showed that 149 units larger than 1MW were connected to DH networks in Europe (for a total of 1580 MW heat produced), and that the technical level of the heat pumps currently available for DH installation is advanced enough to allow an even larger diffusion. In order to obtain high performance heat pumps, it is necessary to exploit heat that is available at low temperature or close to ambient temperatures. In [26], the availability of eight types of heat sources was analyzed: low-temperature industrial excess heat, supermarkets, waste-water, drinking and usage water, groundwater, river, lake, and sea water. The analysis showed that potential sources exist almost everywhere in DH areas and that sea water, when available, represents an important opportunity. Various works in the literature have dealt with installing heat pumps in DH networks, which can also provide important economic benefits. An HP connected to a DH was analyzed in [28], considering air, seawater or groundwater as the evaporating sources. The economic benefit was shown to range from €2500 to €6800 per house, depending on the choice of the evaporating source, economic lifetime and discount rate. In [29] different configurations were analyzed for the integration of the heat pump within the heating and cooling networks. The work concludes that this energy conversion solution could be a cost-efficient solution that can contribute to the decarbonization of the district heating sector.
Ommen et al.[30] compared the performances of five possible heat pump configurations in Combined Heat and Power (CHP) driven DH systems, considering different network temperatures, production technologies and fuels. The analysis clearly showed that a change in the supply temperature has a more significant effect on power production than the modification of the supply temperature, and that a configuration that increases the source temperature up to the supply temperature is a convenient choice. The best option for HPs at the CHP level is to increase the return temperature, which results in the lowest operation cost. As far as the connection of heat pumps is concerned, a study on the installation of heat pumps with a high temperature and a large sized DH was conducted in [31]. Results showed that connecting heat pumps to distribution networks provided a larger Coefficient of Performance (COP) than a transport network, and that a large number of full-load HPs could be reached (3500-4000 instead of 2500-3000).

As discussed in [32], the classic way of controlling P2H plants in DH systems is to balance the heat production and demand. In addition, it is possible to exploit the flexibility of these plants to reduce production costs and/or environmental impacts by providing ancillary services and assisting in the integration of VRES [32]. Most of the previous research analyzed the advantages of exploiting the flexibility of P2H plants at the regional or national level. The available heat sources for use in centralized P2H systems in Denmark were mapped in [26]. The authors reported that the use of centralized HP systems can benefit from the use of electricity during periods of high VRES generation. The potential of P2H plants in the Baltic countries was analyzed in [33]. Results showed that the P2H plant took advantage of the available high renewable production. Another study, set in the North-Eastern part of the United States, analyzed several solutions enabled by P2H technologies in order to take advantage of the electricity surpluses that occurred at the national level [34]. The authors of [35] investigated how the utilization of P2H in DH could increase the VRES market value of Northern European Countries. The flexibility enabled by coupling the DH and electricity sector by means of P2H and a CHP system, was investigated for a future Italian scenario in [36]. The impact of different tax designs on the flexibility enabled by P2H systems combined with centralized thermal storage was studied for the Danish system in [37]. Still in the Danish context, the role of electricity grid tariff schemes for the flexible operation of P2H plants connected to the DH was investigated in [38]. In [39] the flexibility within the thermal networks enabled by the thermal storage tanks and by the thermal network itself is analyzed. The paper defines that although the applications of these methods are still uncommon, these kinds of storages have a great potential to be used to provide flexibility. In [40] the storage potential of a fifth generation district heating and cooling network at very low temperature is exploited to integrate the excess PV generation: this solution was found to be able to absorb about 40% of the PV over-generation of the considered scenario. In [41] a multi-energy system is analyzed in which the electricity sector and the DH sector are connected by means of a heat pump and a combined thermoelectric power plant. The energy flows of the multi-energy system are optimized according to the production of renewable energy and a variable electricity tariff.

1.2. Scientific contribution

To the best of the authors' knowledge, no previous study has investigated the potentials that P2H systems at a local urban level have to balance the over-generations of VRES. The thermal model presented in this paper, being able to accurately simulate the network transients, allows one including the effects of heat pumps on the water thermal mass. This enables the opportunity to correctly exploit the electricity fluctuations within the network, which plays the role of an energy storage. Moreover, the paper presents also the effects on the electrical system, including some analysis regarding the beneficial role of P2H to reduce the reverse power flow from the distribution to the transmission system, considering the actual topology of a real electrical distribution grid. Indeed, in recent years, distributed resources have been becoming increasingly more important for the control and regulation of electrical distribution systems. In line with this trend, the European Union is developing market structures to allow distributed resources to participate in the ancillary services market in order to offer flexibility to Transmission System Operators (TSO) [42]. In the future, as concluded in the SmartNet project [43], these types of services could also be exploited within the distribution network by Distribution System Operators (DSOs) for the local balancing of the electricity system. The flexibility enabled by a multi-energy infrastructure (such as a DH and an electricity grid) could be exploited to handle VRES over-generation at the distribution system level.

This paper analyzes how P2H systems could be inserted into a distribution context as a flexible connection point between the electricity and DH sectors. P2H systems are used for sector coupling for two functionalities: *i*) for high efficiency heat production in a DH system and *ii*) to provide flexibility and absorb local VRES over-generation. A scenario based on real data from the electricity network and the district heating network of the city of Turin (in the north-west of Italy) was considered for this study. Although the scenario is based on the energy system of this specific city, results and conclusions are generalizable to other cities served by high temperature DH networks. Three distinct configurations with different connection points within the electricity distribution system were analyzed. This allowed the research group to enquire into how a different connection point of the distributed resources could affect the performance of the plants. Moreover, two different control strategies were applied: in the first one, the DH heat flows were optimized by maximizing the use of the heat produced by the P2H systems; in the second control strategy, in addition to providing heat to the DH, the P2H systems were used to provide flexibility to the electricity sector. This distributed flexible resource was evaluated from a technical and an economic point of view. Indeed, this study analyzed the energy flows between electricity and the DH sector enabled by the P2H technology, as well as the economic profitability of these plants.

1.3. The structure of the paper

The remainder of the paper is structured as follows. Section 2 describes the analyzed multi-energy scenario, the used mathematical models and the technical and economic assumptions made for the simulation and analysis of the case study. Section 3 reports and discusses the results of the multi-energy system, as analyzed from a technical and economic point of view, whereas Section 4 summarizes the main conclusions of the study.

2. Methods

A multi-energy system, consisting of DH Sub-Networks (SN) and a medium voltage (MV) distribution Electricity Network (EN) and), is here analyzed, in order to establish the benefits of coupling the electricity and district heating sectors at the distribution level (see Figure 1).

The case study presented in this paper is based on the Turin DH, which is linked to more than 5000 buildings (about 60 million m^3). This makes it the largest in Italy and one of the largest in Europe. The network is supplied by two CHP gas plants and storage systems located in different areas of the city. The Turin DH network consists of two interconnected parts: a transport network, which includes large diameter pipes (usually larger than 200 mm) that link the thermal plants to the distribution networks, and 182 distribution networks that connect the transport network to groups of buildings located in the same area of the city. A distribution network was considered in the analysis. The water is currently supplied to buildings at a constant temperature of about 115°C, while the return temperature is between 65°C and 45°C. A future scenario was considered in the analyzed application, where, taking advantages of retrofitting actions on buildings, the supply temperature could be reduced by 20 – 30 °C for most of the winter season (except for the harshest days of the year). Thermal storages (sensible water) have been adopted in the Turin network for peak shaving purposes, especially the morning peak, which occurs after the night switching off. In the considered application, the adoption of thermal storage increases the thermal mass of the system. This provides a significant benefit, since it increases the potential of DH of acting as a source of flexibility for the electricity network. Further developments of the current network are planned, allowing an increase in the volume connected [44]. The expansion of the district heating system will include new distribution networks. The various heat distribution networks can differ considerably from each other (building volumes of different orders: 10^5-10^6 m^3). Nevertheless, it is common to find distribution networks that have similar characteristics in terms of size and type of connected users. In this study, three possible new distribution networks were analyzed, which were hypothesized to have the same thermal characteristics (see Figure 1.). This methodological choice was made in order to evaluate the effects on the thermal sector of different P2H system configurations. More specifically, it was investigated how a different connection point of the P2H plant with the electricity network could modify the performance of the thermal sector and, at the same time, how the same flexible resource could be more or less advantageous for the electricity sector, depending on the specific connection point with the electricity distribution network.

The distribution EN is part of the MV system of the city of Turin. The network is connected to the high voltage (HV) system via three HV/MV transformers (TR). The EN is characterized by a high penetration of VRES. When the VRES production exceeds the electricity demand of the network, the over-generations cause RPF in the HV/MV transformers. The loads and VRES plants are not uniformly distributed within the electricity network (see Figure 2). Most of the VRES systems are installed downstream of TR#2 and TR#3. About half of the electricity network users are connected to the part of the network powered by TR#2. TR#3 is the one most subject to the over-generations of renewables: 70% of VRES over-generations occurs downstream of TR#3, 21% downstream of TR#1, and 9% downstream of TR#2. The connection points of the VRES inside the electricity network are schematized in the Figure 3.

The electricity and the district heating sector are connected though three P2H plants. Each P2H plant is connected downstream of the connection point between the transport district heating network and a district heating distribution network. In particular, the P2H plants are connected to the return flow of the distribution networks. The connection of the P2H plants with the electricity network was defined according to the methodology presented in [45] (which allows an optimal configuration of the distributed energy resources according to the distribution network losses). Each P2H plant is connected downstream of one of the three EN transformers. For the sake of simplicity, the TRs, the P2H systems, the SNs and the ST have been enumerated as shown in Figure 1.

This configuration makes it possible to analyze P2H systems in the three considered positions of the electricity network, which have very different local characteristics: medium local VRES over-generation (P2H#1), low local VRES over-generation (P2H#2) and high local VRES over-generation (P2H#3). As discussed before, the three DH sub-networks to which the P2H plants are connected and the three P2H plants were chosen with the same thermal characteristics (see Table 1). Each SN feeds the thermal demand of an equal volume of buildings. Consequently, the three subnets have an equal heat demand profile (see Figure 4). In this way, the three configurations only differ with respects to their connection points with the EN. The choice of analyzing a scenario with three different plants, three transformers and three DH subnets was made to make the study more general.

P2H absorbs the EN electricity and injects heat into the DH. The P2H plants preheat the return flows of the district heating network, thus decreasing the heat load required by the central system that feeds the district heating. The P2H systems can operate flexibly, thanks to the presence of Thermal Energy Storages (TES) installed at the district heating sub-network level. Moreover, the P2H systems can store the energy taken from the electricity network inside the thermal storages in the form of heat, which can subsequently be used to satisfy the thermal demand of the DH. This scenario has been simulated for one year, with a time resolution of 15 minutes. As described in Section 2.5, two cases were simulated: the first, the Base case, in which the P2H systems only operate as a function of the DH heat needs, and the second, the Optimized case, in which, as before, the P2H systems are used to supply DH heat and, in addition, the flexibility of these systems is exploited to absorb the local VRES over-generations.

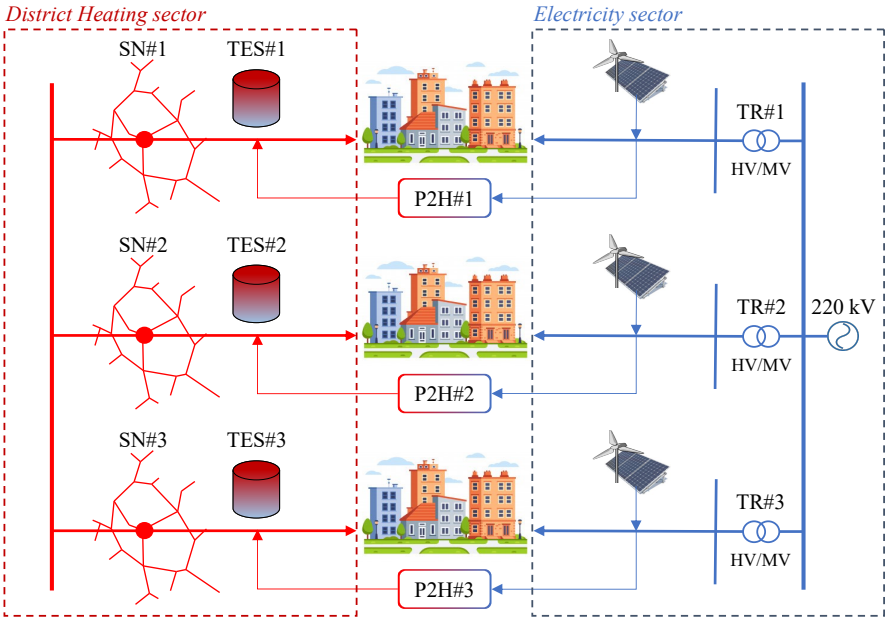

Figure 1. Multi-energy system scenario.

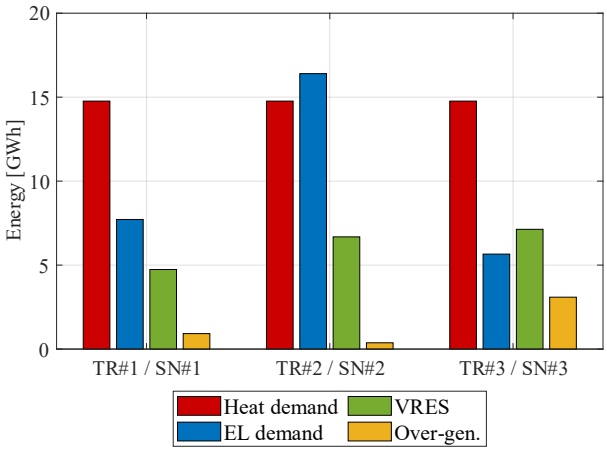

Figure 2. Yearly heat demand, electricity (EL) demand, VRES generation and VRES over-generation (Over-gen.).

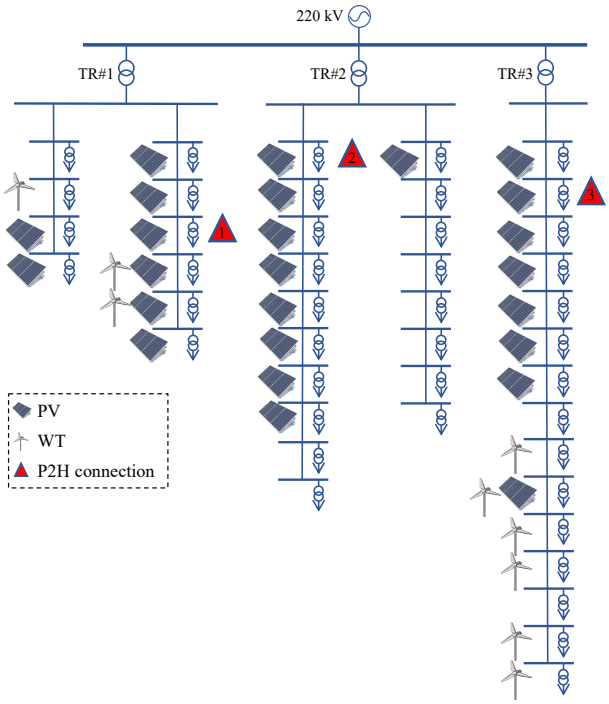

Figure 3. Variable energy sources connection in the electricity network.

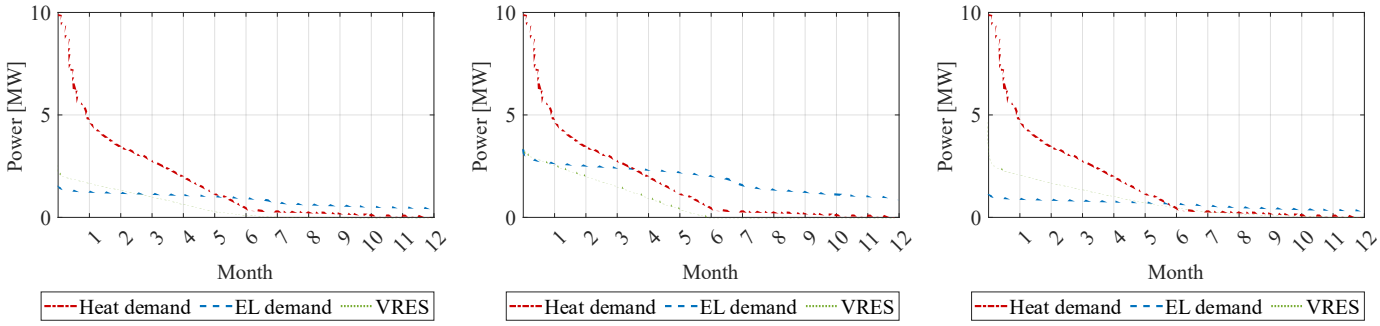

(a) (b) (c)

Figure 4. Duration curve of heat demand, electricity (EL) demand and VRES generation. TR#1 and DH SN#1 (a), TR#2 and DH SN#2 (b), TR#3 and DH SN#3 (c).

Table 1. Multi-energy system parameters.

	Unit	TR#1 / P2H#1 / SN#1	TR#2 / P2H#2 / SN#2	TR#3 / P2H#3 / SN#3
Electricity users	MW_e	5.10	9.30	3.90
PV	MW_e	2.90	4.50	3.30
WT	MW_e	0.60	0	2.70
P2H installed capacity	MW_{th}	2.50	2.50	2.50
TES volume	m^3	250	250	250
Heated volume	m^3	250,000	250,000	250,000

2.1. Mathematical models

This section describes the component models of the multi-energy system. The multi-energy system was simulated with four modules:

- the power grid module,
- the DH network module,
- the P2H system module,
- the control module.

These modules were developed separately and integrated with each other using the co-simulation approach presented in [8] and [46]. Simulating multi-energy systems is a complex mathematical problem as the operation of each component of the system is affected by the behavior of all other components. In the co-simulation approach, the different components of the multi-energy system are simulated on separate simulators that are interconnected via a communication system. In this way it is possible to develop the model of each component independently from the others. Each component can then be developed with the most appropriate mathematical method and simulation software. The time horizon of the simulation (1 year) was discretized in time steps of 15 minutes. Each module simulates the operation of a particular component of the multi-energy system. At the end of the k-th co-simulation step, the modules exchange the information required as input in the successive simulation time step.
Thanks to this approach, different methods to solve the mathematical problem were integrated in a single simulation platform. In the specific case of this study, at every co-simulation step k, the DH network dynamic model calculates the flows on the branches of the network using an internal integration step ϑ (of duration dt); the electricity network model calculates the power flow (steady state condition of the grid) using an iterative calculation for each time step k, i.e., the network equations are calculated for several iterations j until the convergence is reached; in the same way, the P2H model solves the equations for several h iterations until the convergence is reached; finally, the controller models are solved using an algebraic method (see Figure 5).
It is worth noting that the different modules are equivalent to black boxes, which exchange one to each other input-output data every co-simulation time step k, without the necessity for any model to know the internal structure and the calculation method of the other modules.

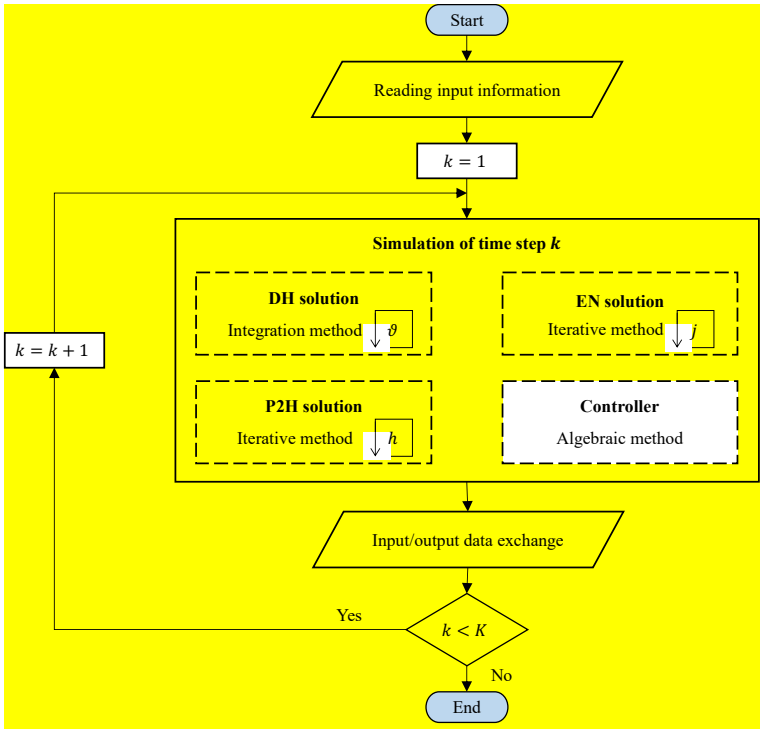

Figure 5. Conceptual flow chart of the overall Co-simulation approach.

2.1.1. District heating network model

A physical model of the network was used to evaluate the temperature within the DH pipelines in order to accurately estimate the impact of P2H on DH. The network model also contains the thermal storage model. The heat flows on the network and the interactions with the storage systems are calculated dynamically with an integration step ϑ. The duration dt of the integration step ϑ has been set in such a way as to allow the convergence of the model to be achieved; in the case study analyzed, the integration step is of the order of 30 seconds.

The DH model allows the contribution of the thermal losses and thermal transients to be taken into account. The model includes mass and energy conservation equations for each junction and each pipe of the network, respectively. These equations were validated in [49]. The model is one-dimensional for each pipe, since the heat propagation follows the main direction of the water flow. A graph approach was used to describe the connection between pipes and junctions. According to this approach, they were considered as branches and nodes. Such an approach is commonly adopted for the description of the topology of a DH network. Specifically, the connection between nodes and branches is described using the incidence matrix (**A**), which has the same number of rows as the number of nodes (N), and the same number of columns as the number of branches (B). A general element, A_{ij}, is equal to 1, or -1, depending on whether the node represents the inlet or outlet of the branch, and 0 if the node is not connected to the branch. This approach allows matrix equations to be written for the entire network. The mass conservation equations written for the nodes and for the entire network are reported in Eq. (1) and Eq. (2), respectively. Eq. (1) states that, at each node, the sum of the entering mass flows must be equal to the sum of the exiting mass flow. From a network perspective, Eq. (2), the sum of the mass flow in each node (achieved by multiplying the incidence matrix by **G**, the matrix of the mass flows in the branches) must be equal to the mass entering or exiting the systems from the external environment $\mathbf{G}_{\text{ext}}$ (e.g., at the thermal plants).

$$\sum_{m=1}^{M_n} G_{n-m}^{(\vartheta)}(k) = 0 \tag{1}$$

$$\mathbf{A} \cdot \mathbf{G}_{\mathrm{B},k}^{(\vartheta)} + \mathbf{G}_{\mathrm{ext}_{\mathrm{N},k}}^{(\vartheta)} = 0 \tag{2}$$

Where:

- M_n is the number of nodes adjacent to node n,
- $G_{n-m}^{(\vartheta)}(k)$ is the mass flow in the branch $n-m$ which connect node n and the adjacent node m at time step k and the iteration of the integration procedure ϑ,
- **A** is the incidence matrix,
- $\mathbf{G}_{\mathrm{B},k}^{(\vartheta)}$ represents the matrix of the mass flows in the branches at time step k and the iteration of the integration procedure ϑ,
- $\mathbf{G}_{\mathrm{ext}_{\mathrm{N},k}}^{(\vartheta)}$ is the matrix containing the mass flow exchanged between the nodes of the network and the external environment at time step k and the iteration of the integration procedure ϑ.

Similarly, the energy conservation equations are reported in Eq. (3) and Eq. (4). The energy conservation equation is written in a transient form since the temperature perturbations within the network travel at the water velocity. This is done since the water keeps long time to reach the thermal plants from the buildings (and vice versa), e.g., order of 30 min- 1h. This means that the time step is much smaller than the phenomena studied, therefore the energy transient should be included in the analysis if temperature gradients are expected to occur. Eq. (3) includes the unsteady term, which represents the thermal capacity of the node, the convective term and, on the right-hand side, the heat generated/losses (which include the contribution of the thermal losses toward the ground).

$$\rho \cdot c_p \cdot \frac{dT_n^{(\vartheta)}(k)}{dt} + \sum_{m=1}^{M_n} \left(\rho \cdot c_p \cdot v_{n-m}^{(\vartheta)}(k) \cdot \nabla T_{n-m}^{(\vartheta)}(k)\right) = \varphi_n^{(\vartheta)}(k) \tag{3}$$

Where:

- ρ is the water density,
- c_p is the water specific heat,
- $\frac{dT_n^{(\vartheta)}(k)}{\partial t}$ indicates the derivative of water temperature in node n at time step k and the iteration of the integration procedure ϑ,
- $v_{n-m}^{(\vartheta)}(k)$ is the velocity of the water flow in the branch $n-m$ at time step k and the iteration of the integration procedure ϑ,
- $\nabla T_{n-m}^{(\vartheta)}(k)$ represents the thermal gradient in the branch $n-m$ at time step k and the iteration of the integration procedure ϑ,
- $\varphi_n^{(\vartheta)}(k)$ represents the specific the heat generated/losses in node n at time step k and the iteration of the integration procedure ϑ.

Integrating and expressing the thermal losses as the product of the global heat exchange coefficient (U_{TOT}) and the temperature difference between the water in the pipe and the temperature of the ground (T_{gr}) it is obtained Eq. (4).

$$\rho \cdot c_p \cdot \frac{dT_n^{(\vartheta)}(k)}{dt} \cdot V_n + \sum_{m=1}^{M_n} c_p \cdot G_{n-m}^{(\vartheta)}(k) \cdot T_{n-m}^{(\vartheta)}(k) = U_{TOT} \cdot (T_n^{(\vartheta)}(k) - T_{gr}) \tag{4}$$

Where V_n is the volume of the node n.
Adopting an Upwind scheme this can be written in matrix form for all nodes. In the matrix form, Eq. (4), the three terms of Eq. (5) are respectively gathered in the mass matrix M, the stiffness matrix K and the known term g.

$$\mathbf{M_N} \cdot \dot{\mathbf{T}}_{\mathrm{N},k}^{(\vartheta)} + \mathbf{K_N} \cdot \mathbf{T}_{\mathrm{N},k}^{(\vartheta)} = \mathbf{g}_{\mathrm{N}}, \forall\ k = 1, \dots, K \tag{5}$$

Where:

- $\mathbf{M}_{\mathrm{N}}$ represents the nodal mass matrix, which includes the terms multiplied for the temperature derivative,
- $\dot{\mathbf{T}}_{\mathrm{N},k}^{(\vartheta)}$ is the vector containing the time derivative of the temperature of the nodes at time step k=1,…,K and the iteration of the integration procedure ϑ,
-
- $\mathbf{K}_{\mathrm{N}}$ represents the stiffness matrix of the network nodes, which includes the terms multiplied for the temperature,
- $\mathbf{T}_{\mathrm{N},k}^{(\vartheta)}$ indicates the vector containing the temperatures of the nodes at time step k and the iteration of the integration procedure ϑ,
- $\mathbf{g}_{\mathrm{N}}$ is the vector containing known terms in the energy equation, which include the terms not multiplied by the temperature or its derivative.

Further details on the model are provided in [49].
The thermal energy storage is connected to the supply network, to store the additional heat produced in the off-peak hours. In particular, this used to provide heat during the morning peak demand (that occurs between 5 am and 7 am). The storage is charged in the night, between 0 am to 5 am, to keep low the thermal losses. During the night, the mass flow circulating in the system is low due to the limited heat demand of the district heating users; in some part of the network (in particular in some distribution networks), water is not circulating. For this reason, due to thermal losses, the temperature inside the network (and within buildings and heating devices) decreases. In the morning, when users request heat from the network, the central system, in addition to providing heat to

the users, must provide the heat necessary to bring the network temperature (and temperature of the heating devices as shown in [50]) back to operating temperature. This causes a peak in district heating heat demand from 5:00 to 7:00. Using the thermal storage allows to decrease the peak demand required from the central plant.
The heat power exchanged with the stage is calculated at each iteration of the integration procedure ϑ as:

$$\Phi_{\mathrm{TES}}^{(\vartheta)}(k) = \mathrm{c}_p \cdot G_{\mathrm{TES}}^{(\vartheta)}(k) \cdot \left(T_{\mathrm{TES},out}^{(\vartheta)}(k) - T_{\mathrm{TES},in}^{(\vartheta)}(k)\right) \tag{6}$$

Where:

- $\Phi_{\mathrm{TES}}^{(\vartheta)}(k)$ is the heat power exchanged with the thermal storage ($\Phi_{\mathrm{TES}}^{(\vartheta)}(k) > 0$ means that the storage inject heat into the DH network, $\Phi_{\mathrm{TES}}^{(\vartheta)}(k) < 0$ means that the storage absorbs heat form the network),
- $G_{\mathrm{TES}}^{(\vartheta)}(k)$ is the water mass flow enhanced with the storage,
- $T_{\mathrm{TES},in}^{(\vartheta)}(k)$ is the temperature of the water flow entering the storage,
- $T_{\mathrm{TES},out}^{(\vartheta)}(k)$ is the temperature of the water output flow.

2.1.2. Power-to-Heat model

The P2H configuration is used to increase the return temperature up to the supply value. The efficiency of P2H is closely related to the temperature of both the heated water and the source side. The P2H energy conversion process is operated by large-scale geothermal HP plants, which exploit the higher temperature of the groundwater to achieve a higher performance.
There is an implicit relationship between the temperature at the exit of the P2H plant, $T_{\mathrm{P2H},out}^{(h)}(k)$, and the exchanged heat flux, $\Phi_{\mathrm{P2H}}^{(h)}$, as shown in Eq. (7): hence, an iterative approach was used to evaluate $T_{\mathrm{P2H},out}^{(h)}(k)$ and $\Phi_{\mathrm{P2H}}^{(h)}$ (out temperature and produced heat evaluated at the iteration h at the time step k) given $T_{\mathrm{P2H},in}$, the *COP*, the water specific heat c_p and the water flow the flow of water passing through the heat pump G_{P2H}.

$$T_{\mathrm{P2H},out}^{(h)}(k) = T_{\mathrm{P2H},in}(k) + \frac{\Phi_{\mathrm{P2H}}^{(h)}\left(T_{\mathrm{P2H},in}(k), T_{\mathrm{P2H},out}^{(h-1)}(k), COP_{\mathrm{P2H}}\right)}{G_{\mathrm{P2H}}(k) \cdot c_p} \tag{7}$$

In order to take the characteristics of the device into account, as well as the operating conditions, the COP was estimated with Eq. (8), adopting the performance of the device in the design condition (taken from the catalogue) and using the Carnot coefficient to simulate performance under real operating conditions.

$$COP_{\mathrm{P2H}} = \epsilon \cdot \frac{T_{\mathrm{P2H},av}(k)}{T_{\mathrm{P2H},av}(k) - T_{\mathrm{P2H},ev}} \tag{8}$$

where:

- $T_{\mathrm{P2H},av}$ is the logarithmic average temperature of the water processed in the P2H plant.
- ϵ is the ratio among the performance of the HP under the design conditions (r) and the Carnot COP under the same conditions ($COP_{CarnotD}$), as shown in Eq. (9),
- in this application, $T_{\mathrm{P2H},ev}$ is the temperature of the groundwater, which can be considered equal to 15°C.

$$\epsilon = \frac{r}{COP_{CarnotD}} \tag{9}$$

2.1.3. Electricity network model

The electricity network analyzed in this case study is radial (the number of nodes without the slack, N, is equal to the number of branches, B). The power flow calculation was solved with the equivalent single-phase Backward Forward Sweep (BFS) algorithm [47]. BFS calculates the current in each branch for each time step, $k = 1, \dots, K$, as in Eq. (10):

$$\begin{cases} \underline{\mathbf{i}}_{\mathrm{B},k}^{(j)} = \mathbf{\Gamma}^{\mathrm{T}} \cdot \underline{\mathbf{i}}_{\mathrm{N},k}^{(j)} = \mathbf{\Gamma}^{\mathrm{T}} \cdot \left[\underline{\mathbf{y}}_{\mathrm{C}} \circ \underline{\mathbf{v}}_k^{(j-1)} + \underline{\mathbf{s}}_k{}^* \oslash \left(\underline{\mathbf{v}}^{(j-1)}\right)^*\right] \\ \underline{\mathbf{v}}_k^{(j)} = \underline{\mathbf{v}}_{0,k} - \mathbf{\Gamma} \cdot \underline{\mathbf{Z}}_{\mathrm{B}} \cdot \underline{\mathbf{i}}_{\mathrm{B},k}^{(j)} \end{cases}, \ \forall \ k = 1, \dots, K \tag{10}$$

where:

- $\underline{\mathbf{i}}_{\mathrm{B},k}^{(j)} \in \mathbb{C}^{B,1}$ indicates the vector that contains the complex currents, for iteration j at time step k,

- $\underline{\mathbf{v}}_k^{(j)} \in \mathbb{C}^{N,1}$ is the vector of the complex voltages, at iteration j at time step k,
- $\underline{\mathbf{i}}_{\mathrm{N},k}^{(j)} \in \mathbb{C}^{N,1}$ represents the vector that contains the load node complex currents, at iteration j;
- $\mathbf{\Gamma} \in \mathbb{N}^{B,N}$ indicates the inverse of the node-to-branch incidence matrix,
- $\underline{\mathbf{y}}_{\mathrm{C}} \in \mathbb{C}^{N,1}$ is the vector that reports the load admittances and the network admittance,
- $\underline{\mathbf{s}}_t \in \mathbb{C}^{N,1}$ represents the vector of the constant power loads at time k, that is, the loads that absorb a constant power whatever the nodal voltage,
- $\underline{\mathbf{v}}_{0,k} = \underline{V}_{\mathrm{slack},k} \cdot \mathbf{u}_{\mathrm{N}}, \underline{\mathbf{v}}_{0,k} \in \mathbb{C}^{N,1}$ indicates the vector filled with the complex value of the slack voltage ($\underline{V}_{\mathrm{slack},k}$) at time step k ($\mathbf{u}_{\mathrm{N}} \in \mathbb{N}^{N,1}$ is the unitary vector),
- $\underline{\mathbf{Z}}_{\mathrm{B}} \in \mathbb{C}^{B,1}$ represents the diagonal matrix that reports the values of the impedances of the network branches,
- K is the number of time steps,
- $\oslash$ and $\circ$ are the Hadamard division and product, respectively,
- * is the conjugate operation.

The electrical network model also calculates, at each step k, the RPF in each transformer of the network, $RPF_{TR\#i}(k)$, as shown in Eq. (11) and Eq. (12).

$$\mathcal{E}_{TR\#i,k} = \tau \cdot real\left(\underline{V}_{\mathrm{slack},k} \cdot \underline{I}^*_{\mathrm{slack},TR\#i,k}\right), \forall\, k = 1, \dots, K \tag{11}$$

$$RPF_{TR\#i,k} = \begin{cases} \mathcal{E}_{TR\#i,k}, & real\left(\underline{V}_{\mathrm{slack},k} \cdot \underline{I}^*_{\mathrm{slack},TR\#i,k}\right) < 0 \\ 0, & \text{otherwise} \end{cases}, \forall\, k = 1, \dots, K \tag{12}$$

where:

- $\mathcal{E}_{TR\#i,k}$ is the electrical energy that flows through the i-th transformer for the time step k,
- τ is the duration of the time step (e.g., 15 minutes),
- $\underline{I}_{\mathrm{slack},TR\#i,k}$, represents the complex value of the current flowing through the i-th transformer for the time step k,

More details on the electricity grid model are reported in [48].

2.1.4 Coordination of the Power-to-Heat flexible resources

The flexibility of the *i*-th P2H is defined by three values at each simulation step (*k*): the electricity base load, the upward flexibility ($\pi^{+}_{P2H\#i}$) and the downward flexibility ($\pi^{-}_{P2H\#i}$) [8].
The base load ($\pi^{0}_{P2H\#i}$) is defined as the electrical consumption of the system, whenever it is used solely to satisfy the needs of the thermal sector: P2H is used to provide as much heat as possible to the DH. To be noted that from 0:00 to 5:00 the P2H units are also used to charge the thermal storages. During these hours the TES are charged with a constant heat flow until reaching the maximum state of charge at 5:00. During the other hours of the day, if the TES is charged, the P2H system is turned off to allow the storage to discharge the accumulated heat until the thermal storage is completely empty. In such a situation, the DH heat demand is met entirely by the heat coming from the storages. When P2H system is operating (to either charge the storage or to supply heat directly to the SN), it must be supported by high temperature heat from the DH transport network, in order to reach the required operating temperature (i.e., 115°C). This is because the P2H system can reach only relatively low temperatures (i.e., 90°C).
The base load of the *i*-th P2H is defined at each simulation step (*k*) according to the flow diagram in Figure 6:

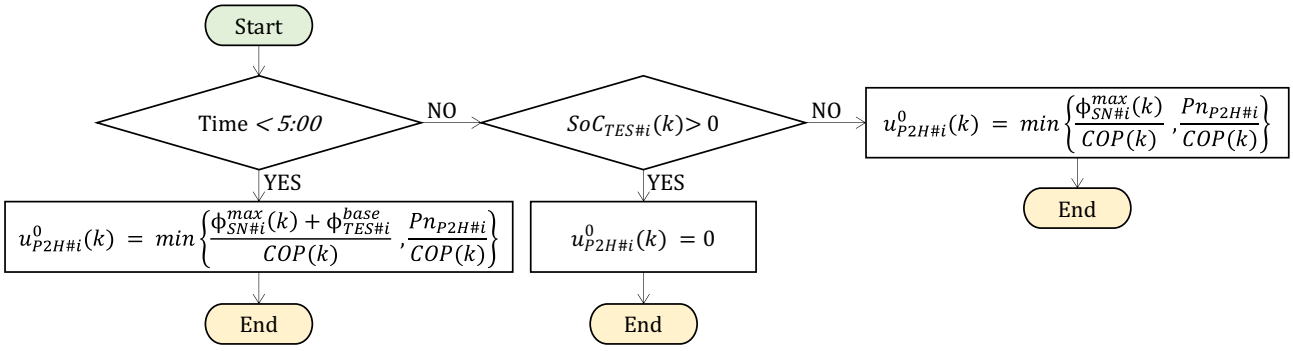

Figure 6. The *i*-th P2H base load control algorithm. Optimization of DH heat flows.

Where

- $\Phi^{max}_{SN\#i}(k)$ is the maximum heat power that the i-th P2H plant can inject into the i-th SN at step k;

- $\Phi_{TES\#i}^{base}(k)$ is the heat that the i-th P2H must provide to the i-th TES to store heat during the charging period and linearly reach the maximum charge at the end of the accumulation period;
- $Pn_{P2H\#i}$ is the nominal heat power of the i-th P2H plant;
- $SoC_{TES\#i}(k)$ is the State of Charge (SoC) of the i-th TES at step k.

Downward flexibility is defined as the maximum allowable downward deviation from the base load. Since, a time interval of 15 minutes has been considered, the electricity consumption of the P2H systems can always be brought to 0. Therefore, the downward flexibility is always equal to the base load, as shown in Eq. (13):

$$\pi_{P2H\#i}^{-}(k) = u_{P2H\#i}^{0}(k) \tag{13}$$

Upward flexibility is defined as the difference between the electrical load of the plant when it works to deliver the maximum amount of heat that can be stored in the DH sector (considering the accumulation in storage) and the base load, as reported in Eq. (14):

$$\pi_{P2H\#i}^{+}(k) = min\left\{\frac{\Phi_{SN\#i}^{max}(k) + \Phi_{TES\#i}^{max}(k)}{COP(k)}, \frac{Pn_{P2H\#i}}{COP(k)}\right\} - u_{P2H\#i}^{0}(k) \tag{14}$$

where $\Phi_{TES\#i}^{max}(k)$ is the maximum heat power that the i-th P2H can inject into the i-th thermal storage system.

Base case: without P2H flexibility exploitation

In the Base case, although the two energy sectors are connected, the synergies enabled by the energy conversion technologies are not exploited. P2H systems only operate to satisfy the needs of the thermal sector. According to the above definition, the P2H plants always work at their base load, as stated in the control logic illustrated in Figure 6.

Optimized case: with Power-to-Heat flexibility exploitation

In the Optimized case, the flexibility of the P2H systems is exploited to control their electricity consumption and optimize the energy flows of the electricity sector. The electrical load of the P2H plants is shifted as much as possible to match the VRES over-generations, and thus reduce the RPF in the network transformers. Figure 7 summarizes the logic adopted to control the P2H plants at the generic time step k. In the absence of VRES over-generation downstream of the i-th transformer, the electrical load of the i-th P2H is kept equal to the base load. If the i-th transformer is subject to an RPF ($RPF_{TR\#i}$), the flexibility of the i-th P2H plant is exploited to absorb as much of the local VRES over-generation as possible.

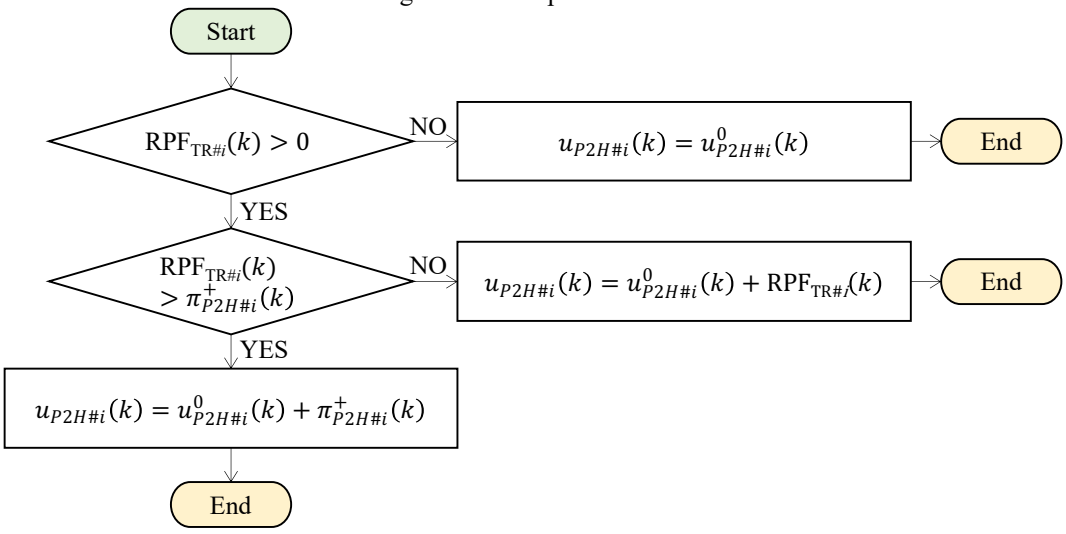

Figure 7. Flexibility exploitation control algorithm of the i-th P2H unit for RPF absorption.

2.2. Economic analysis

This section shows the details and parameters of the economic analysis carried out to evaluate the profitability of the use of P2H plants. In particular, section 2.6.1 shows how the cost and earnings deriving from the use of P2H plants are calculated. Section 2.6.2 summarizes the assumptions regarding the P2H plant investment cost and its maintenance. Finally, section 2.6.3 shows how the economic performance parameters were calculated.

2.2.1. Energy costs and incentives for flexibility

The average price of the electricity consumed by the P2H plants was estimated to be 60 €/MWh. The heat generated by the plants was estimated to be worth 45 €/MWh. Indeed, the heat injected into the DH represents a source of revenues, as it brings about a reduction in the central CHP usage, thus reducing the associated costs. Until now, the flexibility offered at the distribution level has not been regulated. For this reason, a sensitivity analysis was performed: by varying the value of incentives from 0 to 60 €/MWh, the impact of these incentives on the cash flow of P2H plants has been investigated.

The energy costs and the incentives for the provided flexibility are summarized in Table 2.

Table 2. Flexibility incentives and energy costs

Parameter	Unit	Value
Average electricity cost	€/MWh$_e$	60
Heat cost	€/MWh$_{th}$	45
Incentives for flexibility	€/MWh$_e$	0 – 60

2.2.2. Power-to-Heat plant cost assumption

The investment cost includes the HP purchase cost and the excavation/installation costs for the sink construction. Indications of the total cost of various kinds of existing large scale HP projects (depending on the heat source and HP capacity) are reported in [51]. An investment cost of 700-1100€/kW$_{th}$ is indicated for the specific case of a groundwater HP. According to [52], the investment cost for a large scale P2H plant will decrease by 10% in 2030 and by 16-20% in 2050. This expected cost reduction will not be caused by an energy efficiency improvement, as this technology is already well known and fully developed. Nevertheless, the use of large HP plants connected to the DH is still not particularly widespread. In the future, the penetration of this technology is expected to increase, with a consequent decrease in the production cost of the components due to a scale effect. In this study, an investment cost of 770€/kW$_{th}$ has been considered, while, according to [37], the fixed operational and maintenance (O&M) costs were assumed be equal to 2€/(kW$_{th}$·year) and the plant lifetime equal to 25 years (see Table 3).

Table 3. Power-to-Heat plant cost assumptions.

Parameter	Unit	Value
Investment cost	€/kW$_{th}$	770
Fixed O&M cost	€/(kW$_{th}$·year)	2
Lifetime	years	25

2.2.3. Simple pay back and Net Present Value

The economic flows of P2H plants are assessed on the basis of the electricity consumed, the heat produced, and the flexibility provided, which are calculated as shown in Eqs. (15-17)

$$Cost_{el,P2H\#i} = c_{el} \sum_{k=1}^{\mathrm{K}} u_{P2H\#i}(k) \cdot \tau \tag{15}$$

$$Rev_{heat,P2H\#i} = r_{heat} \sum_{k=1}^{\mathrm{K}} \Phi_{P2H\#i}(k) \cdot \tau \tag{16}$$

$$Rev_{flex,P2H\#i} = r_{flex} \sum_{k=1}^{\mathrm{K}} \left(u_{P2H\#i}(k) - u^0_{P2H\#i}(k) \right) \cdot \tau \tag{17}$$

where:

- $Cost_{el,P2H\#i}$ represents the annual expenses for the electricity consumption of the i-th P2H plant,
- c_{el} is the annual average price of electricity,
- $Rev_{heat,P2H\#i}$ indicates the annual revenues for the heat production of the i-th P2H plant,
- r_{heat} is the specific revenue for the heat injected into the DH,
- $Rev_{flex,P2H\#i}$ represents the annual revenues for the flexibility provided by the i-th P2H plant. The reader may appreciate that this kind of revenue is not available in the base case as the flexibility of the P2H plants is not exploited (i.e., $u_{P2H\#i}(k) = u^0_{P2H\#i}(k), \forall\, k = 1, \dots, \mathrm{K}$),
- r_{flex}, represents the specific incentives for the provided flexibility.

The annual cash flows (CF) of the P2H plants were determined by considering four factors: the earnings from the production of heat, the earnings from the flexibility provided, the costs for the consumption of electricity, and the fixed operational expenditure (OPEX), see Eq. (18).

$$CF_{P2H\#i} = Rev_{Heat,CP2H\#i} + Rev_{flex,CP2H\#i} - Cost_{electricity,CP2H\#i} - \mathrm{OPEX}_{CP2H\#i} \quad (18)$$

The P2H plants were evaluated, from an economic point of view, by means of the calculation of the NPV, Eq. (19), and SPB, Eq. (20).

$$NPV_{P2H\#i} = -CAPEX_{P2H\#i} \sum_{t=0}^{Lifetime} \left(\frac{OPEX_{P2H\#i}}{(1-DR)^t}\right) \quad (19)$$

$$SPB_{P2H\#i} = \frac{CAPEX_{P2H\#i}}{CF_{P2H\#i}} \quad (20)$$

Where:

- $CAPEX_{CP2H\#i}$ is the capital expenditure of the i-th P2H plant (considered only at year 0),
- DR is the discount rate, which is assumed to be equal to 6%.

3. Results and discussion

This section reports the results of the analyzed multi energy system scenario. In particular in section 3.1 the energy flows of the multi-energy system are reported and discussed. While section 3.2 shows the economic evaluations of the P2H plants.

3.1. Energy flows between the electricity and district heating energy sectors

In order to illustrate the impact of the two different control strategies (Base case and Optimized case) on the multi-energy system, in this section the energy flows obtained in the two cases are compared (see Figures 8-11).
In the Base case, P2H plants were controlled to optimize the energy flows in the thermal sector. The energy flows in the electricity sector and the thermal sector of a characteristic day with a high heat demand are shown in Figure 8 (details pertaining to mid-February). Since the three DH subnetworks of the scenario have the same characteristics, the heat demand profile is the same for all three subnetworks. The P2H units are used from 0:00 to 5:00 to charge the thermal storage (light green area). Because of the limited temperature that can be reached (90°C), the HPs alone are not able to charge the thermal storage, whose accumulation temperature is 118°C. The storage charge is therefore supported by the heat coming from the transport DH network (called Central Heat: CH in the figures - light gray area). The storage is loaded linearly at night until it reaches the maximum charge at 5:00. In the following hours, the accumulated heat is used to cover the peak of the morning heat demand (orange area). The heat accumulated in the storage, being at a high temperature, is able to satisfy the thermal demand of the network, without needing to take additional heat from the DH transport network. Once the storage is empty (SoC = 0), the P2H plants are again put into operation to supply as much heat as possible to the DH network. The HP plants are used to preheat the return flows of the thermal utilities of the network, thus reducing the heat load required by the central heat power plant. The central plant supplies heat to the return flows, preheated by the P2H plants, up to the operating working temperature of the DH. The heat from the central system is highlighted in dark gray in the figures.
Figure 8b shows the electricity flows that occur downstream of the electricity network's transformers. The dashed line shows the VRES production within the network; it can be seen that TR#3 is the one that is affected the most by over-generation. The flexibility of the P2H plants is not exploited to absorb VRES generation in the Base case. The load of the P2H systems is distributed, during the day, only to satisfy the needs of the thermal sector (red area).
Figure 9 shows the heat and electricity energy flows for the same day in the Optimized case in which the flexibility of the P2H plants is exploited. Until there is no over generation of VRES, the energy flows obtained in the Optimized case are the same as those obtained with the control algorithm of the Base case. In the Optimized case, the electrical load of the P2H plants is controlled to follow the VRES over-generation and mitigate the RPF that adversely affects the network TRs: the P2H plants are used to convert excess electrical energy into heat to be stored in thermal storage. Figure 9b shows the electric power flows that occur in the three electrical network transformers The overproduction in TR#1 and TR#2 is completely absorbed, while the over-generation in TR#3 (of greater entity) is not completely absorbed, thus leaving a residual RPF. P2H#3 cannot absorb all the over-generation of VRES, as it has already reached its nominal capacity load. The optimized control of P2H systems also has an effect on the thermal sector. Indeed, it can be seen that, in the middle of the day (12-15 for SN#1 and SN2, 10-15 for SN#3), when the VRES over-generation occurs, the heat generated by the P2H plants increase compared to the Base case. In these hours the VERS surplus energy is accumulated in the thermal storages (see Figure 9a). In the period immediately following the over-generation of VRES, the thermal demand of the users is completely covered by the storage heat; see, for example, the orange area for SN#3 from 15:00 to 18:00. From the electrical network point of view, the Optimized control logic allows the load of the P2H units to be shifted so as to match the local VRES production. For example, the electricity consumption of P2H#3, which would have been from 15:00 to 18:00 using

the base control algorithm (see Figure 8b), is anticipated and redistributed in a controlled manner during the VRES peak thanks to the optimized control logic (see Figure 9b).

Figure 10 and Figure 11 show the energy flows for a characteristic day with a low heat demand (end of September) for the Base case and the Optimized case, respectively. The heat demand is much lower than that in the winter case (see Figure 10a). Nonetheless, the morning peak demand remains almost constant. In this period of the day, the water inside the network, which is at a low temperature due to the limited energy flows at night, must be brought back to the operating temperature of the network, with a consequent significant heat demand. The morning peak is covered again using the heat accumulated during the night. In the Base case, the P2H load is more concentrated at night for the storage charge, due to the low heat demand in the central hours of the day, and during the evening, when user's heat demand is higher. The electricity consumption profile of the P2H plants is therefore out of phase with the VRES generation, whose peak production occurs in the central hours of the day (see Figure 10b). The flexible use of P2H plants makes it possible to shift part of the electricity consumption to the VRES over-generation hours (see Figure 11b). The energy over-generation that afflicts TR#1 and TR#2 is completely absorbed on the day reported in the figure, while only a part of the over-generation in TR#3 is absorbed. The absorption of the RES over-generation on TR#3 is blocked at 13:00, as the thermal storage has reached its maximum state of charge and is no longer able to accumulate energy. The reader may note that the heat accumulated in TES#1 and TES#3 is not completely released to the DH during the day (the SoC of the two storage units is greater than 0 at the end of the day, see Figure 11a). The heat that remains accumulated in the storage at the end of the day is used the following day. Even for the day before the one represented in Figure 11, TES#1 and TES#3 are not completely discharged at the end of the day. In fact, as can be seen in Figure 11a, the SoC of the two storages at 0:00 is greater than 0. The heat accumulated in the previous day is used to decrease the energy consumption used for night storage charging; the night energy consumption (thermal and electrical) in Figure 10 should be compared with that in Figure 11.

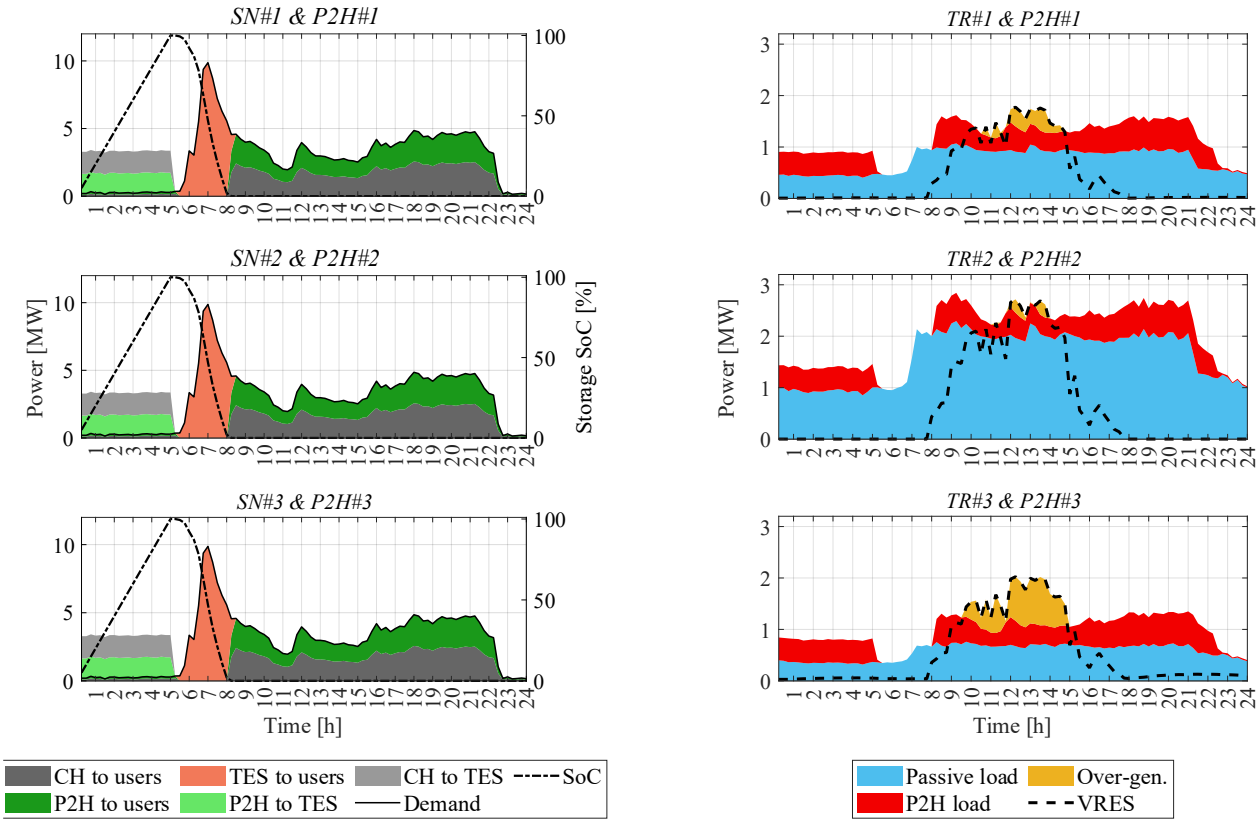

(a) (b)

Figure 8. Base case energy flows in each DH subnetwork (a) and in each transformer (b). Details of a day with a high DH heat demand (February).

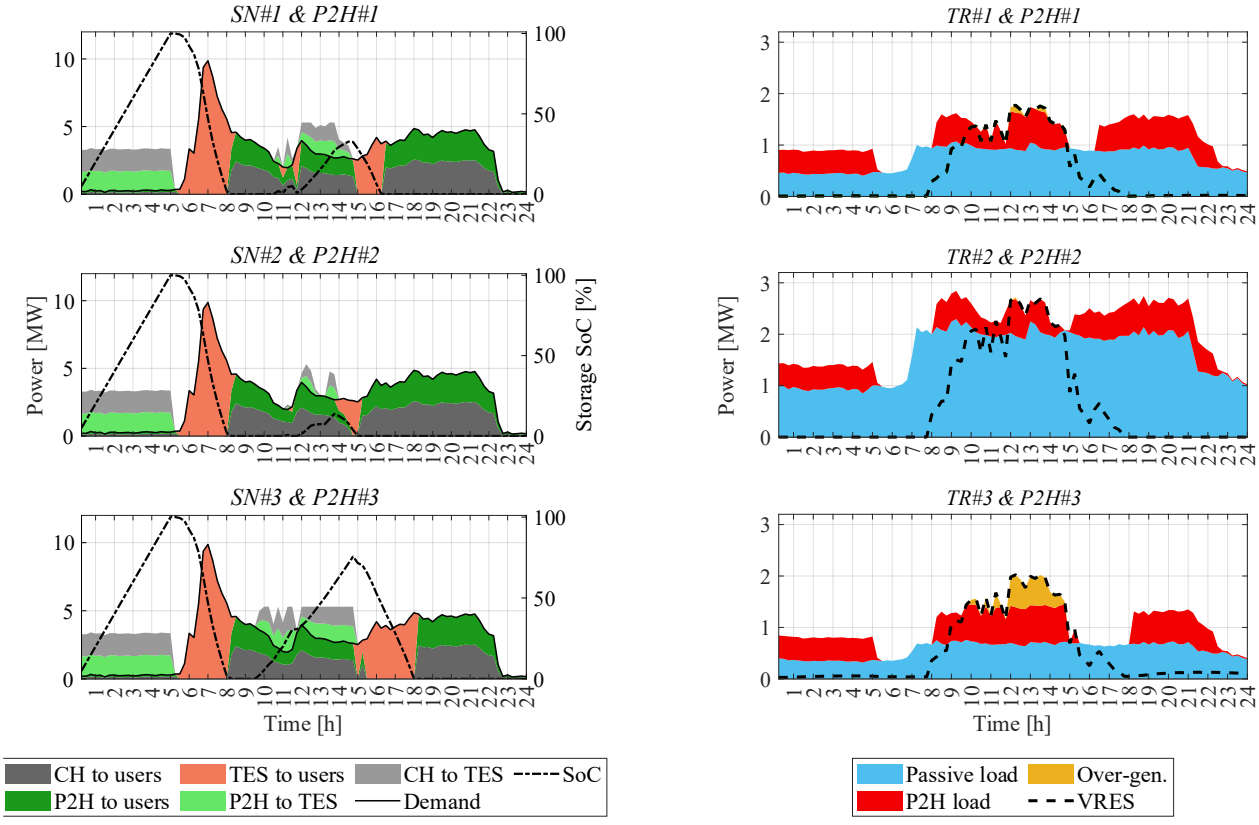

(a) (b)

Figure 9. Optimized case energy flows in each DH subnetwork (a) and in each transformer (b). Details of a day with a high DH heat demand (February).

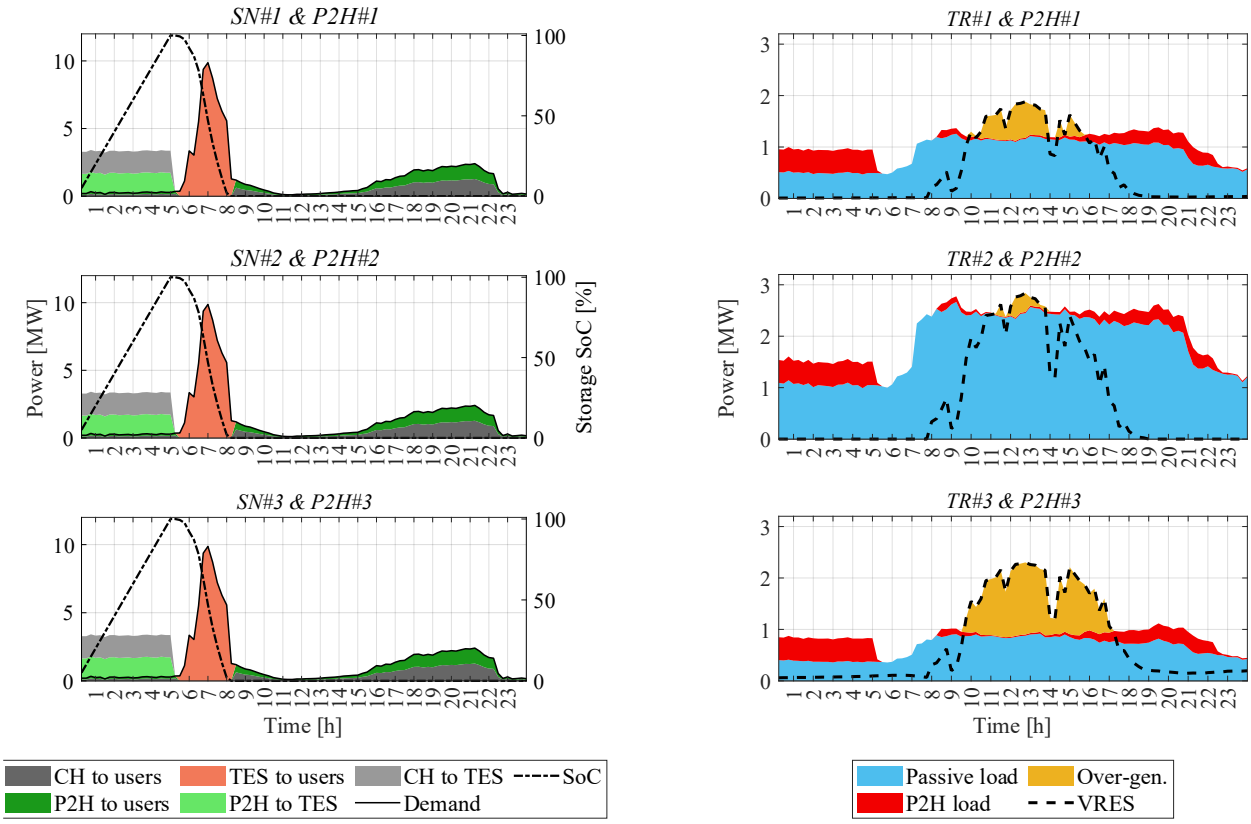

(a) (b)

Figure 10. Base case energy flows in each DH subnetwork (a) and in each transformer (b). Details of a day with a low DH heat demand (September).

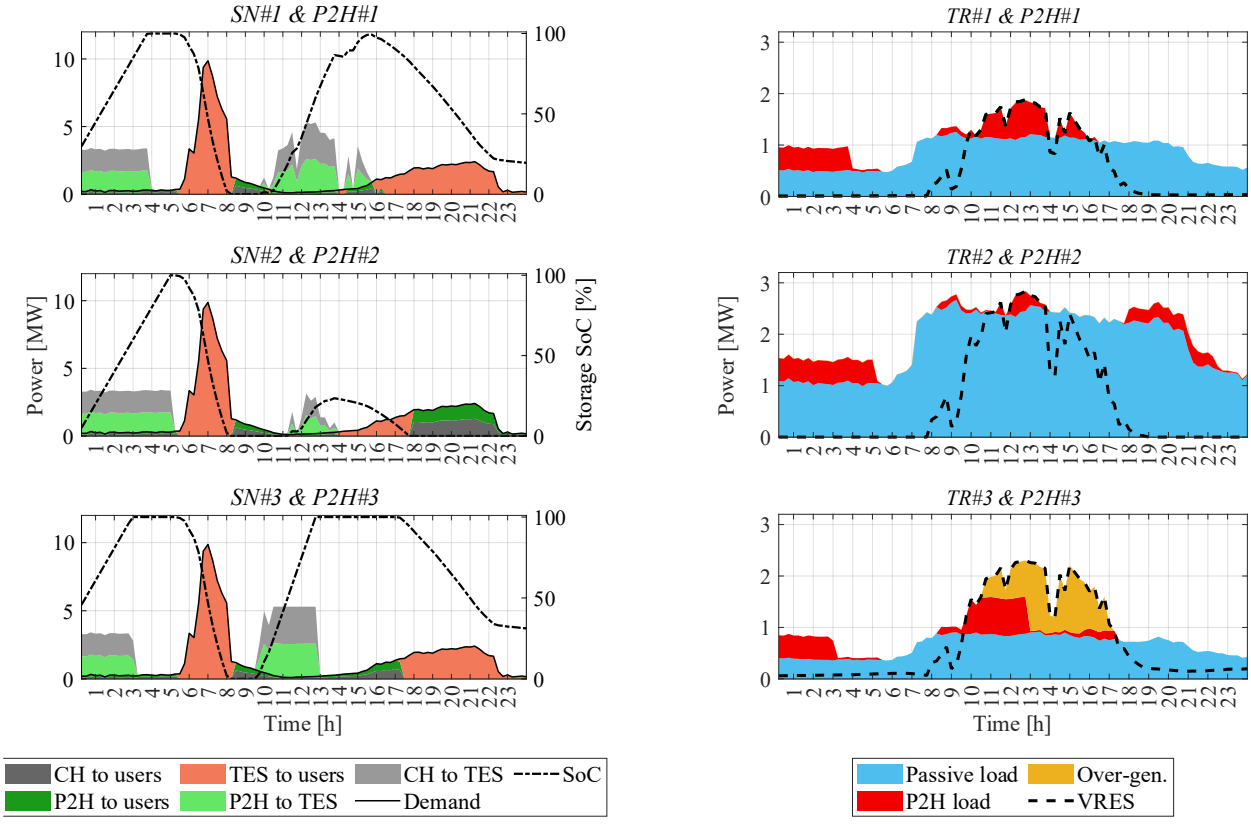

(a) (b)

Figure 11. Optimized case energy flows in each DH subnetwork (a) and in each transformer (b). Details of a day with a low DH heat demand (September).

Table 4 reports the annual energy flows of the three DH subnetworks considered in the Base case for the Optimized case. The table shows:

- the total heat demand of each thermal SN,
- the heat supplied to the users produced directly by the central heat system,
- the heat of the P2H used directly to provide heat to the users,
- the heat that the central system and the P2H plants accumulate in the TES, respectively,
- the total heat that is absorbed and then released by the TES plants.

As mentioned above, the three thermal subnetworks in the Base case behave in the same way, having the same characteristics. A total of 33% of the heat supplied to users is supplied directly by the CH plant, 29% is supplied directly by the HPs, and the remaining 38% comes from thermal storage. In turn, 53% of the heat accumulated in the thermal storage comes from the DH central heating system and the remaining 47% from the P2H plants.
The possibility of decoupling the heat demand from the production enabled by thermal storage is exploited in the Optimized case. The heat accumulated in the storage, which is produced by the centralized heat plant and the P2H plants, increases. Conversely, the heat that is supplied directly to the users (i.e., without first passing through the storage), which comes from the thermal power plant and the P2H systems, decreases. It should be noted that both the total heat coming from the thermal power plant (CH to users + CH to TES) and the total heat produced by P2H (P2H to users + P2H to TES) remain unchanged, compared to the Base case. The flexible use of the P2H system, in fact, does not change the amount of energy required. Instead, it brings about a production time-shift, which is made possible by the passage of energy through the storage systems. The greater the exploitation of the flexibility of the P2H systems, the greater the use of the storage systems. In the analyzed scenario, SN#3 is the one that is most exploited to offer flexibility. As a result of the flexible use of storage, the thermal energy that is accumulated annually in TES#3 increases by 32%, compared to the Base case. The energy that is accumulated in TES#1 and TES#2, whose flexibility is exploited to a lesser extent, increases, due to the flexible use of 29% and 18% of energy, respectively, compared to the Base case.

Table 4. Annual energy flows of the district heating network.

	Unit	**SN#1**		**SN#2**		**SN#3**	
		Base Case	Opt. Case	Base Case	Opt. Case	Base Case	Opt. Case
Heat demand	GWh_{th}	14.77	14.77	14.77	14.77	14.77	14.77
CH to user	GWh_{th}	4.83	3.96	4.83	4.30	4.83	3.88
P2H heat to user	GWh_{th}	4.31	3.53	4.31	3.84	4.31	3.46
CH to TES	GWh_{th}	2.97	3.84	2.97	3.50	2.97	3.93
P2H heat to TES	GWh_{th}	2.65	3.43	2.65	3.13	2.65	3.50
TES heat	GWh_{th}	5.62	7.27	5.62	6.63	5.62	7.43

Thanks to the exploitation of flexibility, the P2H load is shifted to the VRES production hours. Table 5 shows that the quantity of VRES consumed by the network increases and the imported energy (i.e., withdrawn from the HV system) decreases. The greater the surplus is, the more the electricity load can be shifted and, in turn, the lower the electricity withdrawn from the transmission system. Thanks to the flexible use of P2H plants, it is possible to absorb 1.37 GWh of VRES over-generation (about 40% of the total over-production of the entire grid). The amount of energy taken from the HV system decreases by the same amount, as the over-generation VRES decreases. In fact, the total load of the P2H plants is not modified, and is only shifted from the periods of low VRES production to the periods of high VRES production.
The part of the network downstream of TR#3 is the one with the greatest over-generation of VRES (see Table 5). Consequently, the amount of over-generation that have been absorbed by P2H in this part of the network is also the greatest: 0.67 GWh_e, calculated as the over-generations in the Base case minus the over-generations in the Optimized case. The over-generations absorbed by TR#1 and TR#2 are instead 0.48 GWh_e and 0.22 GWh_e respectively. Despite the fact that a greater over-generation of VRES in absolute terms, is mirrored by a greater amount of over-generation absorbable by the flexible units, the effect is the opposite in percentage terms: thanks to P2H units, it is possible to absorb 65% of the over-generations that affect TR#1, 73% of those that affect TR#2 and only 26% of those that affect TR#3. In fact, the flexibility of P2H is limited by two constraints: the P2H nominal load and the state of charge of the storage system. The greater the required flexibility is, the more frequent are the periods during which the unit works at nominal load, thereby limiting the ability to absorb more over-generations of VRES. Moreover, when a greater flexibility and greater amount of energy to inject into the storage are required, there is an increase in the periods in which the P2H plant cannot provide flexibility, as the storage has reached the maximum state of charge.

Table 5. Annual energy flows of the electricity network.

	Unit	**TR#1**		**TR#2**		**TR#3**	
		Base Case	Opt. Case	Base Case	Opt. Case	Base Case	Opt. Case
Electricity demand	GWh_e	7.72	7.72	16.40	16.40	5.65	5.65
P2H load	GWh_e	2.00	2.00	2.00	2.00	2.00	2.00
Electricity withdrawn	GWh_e	5.72	5.24	12.02	11.80	3.05	2.38
VRES consumption	GWh_e	4.00	4.48	6.38	6.60	4.60	5.27

VRES over-gen.	GWh_e	0.74	0.26	0.30	0.08	2.53	1.86

3.2. Economic results

Table 6 shows the electricity consumption, production and annual flexibility provided by the three P2H plants for both the Base and Optimized case. The total production of heat and the total electrical consumption of the three units is the same. Since all three DH subnetworks have the same characteristics, the quantity of heat that P2Hs can provide and, consequently, their electricity consumptions are the same. The optimized use of the flexible units allows the load of the units to be shifted over time and enables flexibility of the plants, without altering their annual energy production or consumption. The plant located downstream of TR#3 is the one that provides the greatest amount of flexibility. The other two plants are located in less advantageous positions, and hence they are less frequently used to offer flexibility. The exploitation of flexibility affects the economic flows of the plants: the greater the flexibility provided by the plant is, the greater are the revenues for the related incentives.

In the hypothesis of 0 incentives (value of incentives = 0 €/MWh), the economic revenues are exclusively derived from the production of heat (equal for all the plants). Under this hypothesis, all three plants are subjected to the same economic flows, which correspond to the economic flows of the Base case, in which flexibility is not exploited. The NPV of all the plants is €670,000 with an SPB of 10.2 years (see Figure 12a and Figure 12b).

The economic benefits derived from the flexible use of the P2H facilities can be appreciated when flexibility incentives have values higher than 0. The greater the incentives are, the greater the economic profitability of these plants (i.e., their NPVs) when their flexibility is exploited. On the other hand, the variation of the incentive parameter in the Base case does not change the economic flows, since the provided flexibility is always zero (see Figure 12a).

From an economic point of view, the best results are those pertaining to P2H#3. In the most optimistic hypothesis on the value of incentives (60 €/MWh), the exploitation of flexibility allows the NPV of P2H#3 to increase by 82% and the SPB to decrease by 18%. The exploitation of flexibility also allows the other two plants to improve their economic flows, even though to a lesser extent. In the most favorable incentive conditions, compared to the Base case, the NPV of plants 1 and 2 increases by 59% and 30% respectively, and the SPB decreases by 13% and 7%.

It should be pointed out that the installation of a P2H system is always convenient, even when flexibility is not exploited. The gains that can be derived from the production of heat compensate for electricity and investment costs. Nevertheless, economic profitability increases significantly if the flexibility of the plants is exploited. In this case, the placement of the P2H plant within the electricity network plays a significant role. In order to maximize the economic revenues, the P2H plant should be located close to the local VRES over-generations. In fact, the greater the over-generations that the plant can absorb are, the greater the flexibility that the plant can provide, with a consequent increase in the revenues for the related incentives. In the analyzed scenario, the NPV of P2H#3, the one that is positioned the best, is as much as 40% higher than the NPV of P2H#2.

Table 6. Annual energy flows of P2H.

	Unit	**TR#1**		**TR#2**		**TR#3**	
		Base Case	Opt. Case	Base Case	Opt. Case	Base Case	Opt. Case
P2H load	GWh_e	2.00	2.00	2.00	2.00	2.00	2.00
P2H flexibility	GWh_e	0.00	0.48	0.00	0.22	0.00	0.67
P2H heat	GWh_{th}	6.96	6.96	6.96	6.96	6.96	6.96

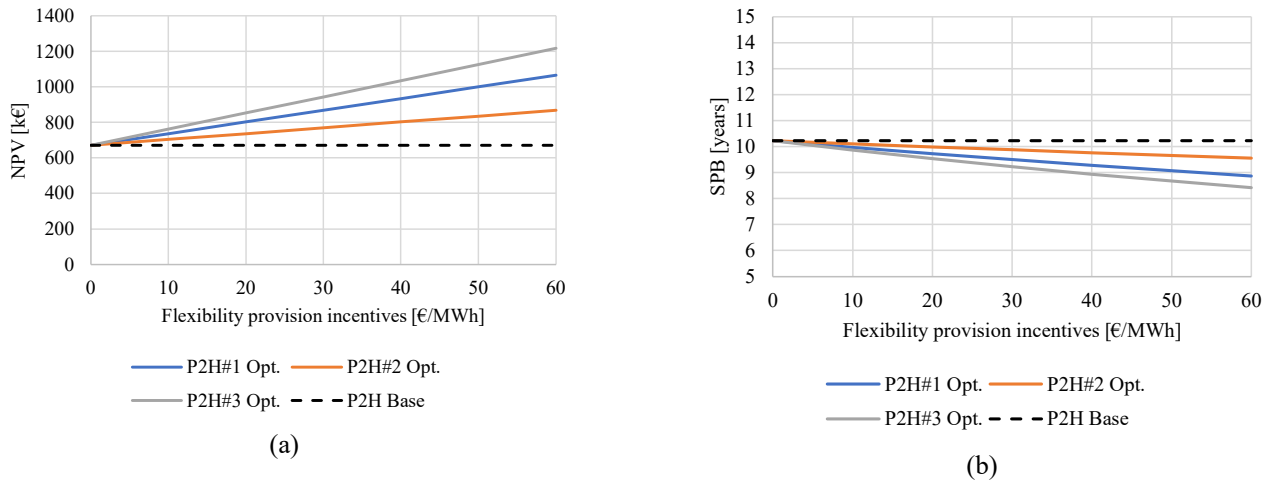

(a) (b)

Figure 12. Net Present Value (a) and Simple Pay Back (b) of the three P2H plants for the Base case and for the Optimized case.

4. Conclusions

This article investigated the concept of using DH connected P2H systems. Three benefits arise from using P2H systems: *a*) first, the use of HP plants represents an efficient solution for the production of heat, *b*) second, these plants can be powered directly by renewable sources, thus allowing the production of heat with a low environmental impact, and *c*) third, the P2H energy conversion technology makes it possible to transfer the flexibility of the district heating sector to the electricity sector. A case study, based on data from the DH and electricity network of the city of Turin, was analyzed The actual implementation of the strategies presented in the paper requires the introduction of a communication system allowing the heat pumps to receive the setpoints and to dialogue with the system operator (through an aggregator, as specified for example in [53]). This can be based on wireless communication and use IEC 62325 for the exchange of the market information between the trading system and the market-place, and IEC 60870-5-104 for the telecontrol of the heat pumps. The last one is well established and diffuse in Asia and Europe at distribution level, even though the use of the protocol IEC 61850 is expected to grow and wide the fields of use in the future, and hence may substitute it [54].The energy flows between the electricity and DH sectors, made possible by the P2H energy conversion technology, were analyzed.

The main conclusions can be summarized as follows:

- In the analyzed scenario, the heat produced by the P2H plants could cover about 50% of the DH heat demand. However, the heat demand cannot be completely satisfied by P2H systems, due to the limited output temperature this technology reaches (a HP capable of reaching 90°C was considered in this study). However, the current Turin district heating network works at a temperature of about 115°C. For this reason, the heat generated by heat pumps should always be integrated by heat generated at high temperatures to reach the working temperature of the network.
- The flexibility enabled by P2H plants was used to absorb the over-generation of VRES that occurred at the distribution level, which could cause RPF problems in HV/MV transformers. The P2H plants allowed the VRES over-generations to be reduced by 40% over the whole year.
- Thanks to the high efficiency of heat production, P2H systems proved to be advantageous from an economic point of view. Even in the most disadvantageous analyzed case, i.e., without any incentives for providing flexibility, the investment cost of building a P2H plant was found to be economically positive, with a simple payback time of approximately 10 years. The exploitation of P2H flexibility allows the economic profitability of the plant to be increased. In the most favorable analyzed case, the use of flexibility made it possible to increase the NPV of the plant by about 82% and to reduce the SPB by about 20%.
- Although all the analyzed P2H units were connected to the same electricity distribution network, the location of the flexibility units had a considerable impact on the P2H plants' performance. In order to maximize the economic profitability of the plant, it would be necessary to place the P2H plant downstream of the transformer that is affected the most by VRES over-production. In the analyzed scenario, the optimal positioning of P2H within the electricity network could yield a 40% increase in profitability.

Thanks to their high conversion efficiency, heat pumps will play a fundamental role in the electrification of the heating sector necessary for decarbonization objectives. Nonetheless, in order to maximize the benefits that this technology can offer, it is necessary to take advantage of its flexibility enabled by the coupling of the thermal sector and the electricity sector. Flexibility that will be increasingly necessary in future energy scenarios characterized by a high penetration of variable renewable energy sources in distribution systems.

References

[1] Intergovernmental Panel on Climate Change IPCC. AR6 Climate Change 2021: The Physical Science Basis. Available online at: https://www.ipcc.ch/report/ar6/wg1/.

[2] Meinshausen M, Meinshausen N, Hare W, Raper SC, Frieler K, Knutti R, Frame DJ, Allen MR. Greenhouse-gas emission targets for limiting global warming to 2 C. Nature. 2009;458(7242):1158-62. https://doi.org/10.1038/nature08017.

[3] European Commission. Clean energy for all Europeans. Luxembourg (Belgium) 2019. https://doi.org/10.2833/9937.

[4] Impram S, Nese SV, Oral B. Challenges of renewable energy penetration on power system flexibility: A survey. Energy Strategy Reviews. 2020;31:100539. https://doi.org/10.1016/j.esr.2020.100539.

[5] Cipcigan LM, Taylor PC. Investigation of the reverse power flow requirements of high penetrations of small-scale embedded generation. IET Renewable Power Generation. 2007;1(3):160-6. https://doi.org/10.1049/iet-rpg:20070011.

[6] CEDEC, Eurogas, GEODE. Flexibility in the Energy Transition: A Toolbox for Gas DSOs. 2016. Available online at: https://eurogas.org/media_centre/reports-flexibility-for-the-energy-transition-a-toolbox-for-electricity-and-gas-dsos/.

[7] Diaz-Londono C, Correa-Florez CA, Vuelvas J, Mazza A, Ruiz F, Chicco G. Coordination of specialised energy aggregators for balancing service provision. Sustainable Energy, Grids and Networks. 2022;32:100817. https://doi.org/10.1016/j.segan.2022.100817.

[8] Badami M, Fambri G, Mancò S, Martino M, Damousis IG, Agtzidis D, Tzovaras D. A decision support system tool to manage the flexibility in renewable energy-based power systems. Energies. 2020;13(1):153. https://doi.org/10.3390/en13010153.

[9] Li N, Uckun C, Constantinescu EM, Birge JR, Hedman KW, Botterud A. Flexible Operation of Batteries in Power System Scheduling with Renewable Energy. IEEE Transactions on Sustainable Energy. 2016;7:685–96. https://doi.org/10.1109/TSTE.2015.2497470.

[10] Simão M, Ramos HM. Hybrid pumped hydro storage energy solutions towards wind and PV integration: Improvement on flexibility, reliability and energy costs. Water. 2020;12. https://doi.org/10.3390/w12092457.

[11] Amoli NA, Meliopoulos APS. Operational flexibility enhancement in power systems with high penetration of wind power using compressed air energy storage. 2015 Clemson Univ. Power Syst. Conf. PSC 2015, Clemson, SC, USA: IEEE; 2015. https://doi.org/10.1109/PSC.2015.7101694.

[12] Lund H, Østergaard PA, Connolly D, Ridjan I, Mathiesen BV, Hvelplund F, et al. Energy storage and smart energy systems. International Journal of Sustainable Energy Planning and Management. 2016;11:3–14. https://doi.org/10.5278/ijsepm.2016.11.2.

[13] Chicco G, Riaz S, Mazza A, Mancarella P. Flexibility from Distributed Multienergy Systems. Proc IEEE. 2020;108:1496–517. https://doi.org/10.1109/JPROC.2020.2986378.

[14] Lund PD, Mikkola J, Ypyä J. Smart energy system design for large clean power schemes in urban areas. Journal of Cleaner Production. 2015;103:437-45. https://doi.org/10.1016/j.jclepro.2014.06.005.

[15] Badami M, Fambri G. Optimising energy flows and synergies between energy networks. Energy. 2019;173:400–12. https://doi.org/10.1016/j.energy.2019.02.007.

[16] Diaz-Londono C, Colangelo L, Ruiz F, Patino D, Novara C, Chicco G. Optimal strategy to exploit the flexibility of an electric vehicle charging station. Energies. 2019;12(20):3834. https://doi.org/10.3390/en12203834.

[17] Fambri G, Diaz-Londono C, Mazza A, Badami M, Weiss R. Techno-economic analysis of Power-to-Gas plants in a gas and electricity distribution network system with high renewable energy penetration. Applied Energy. 2022;312:118743. https://doi.org/10.1016/j.apenergy.2022.118743.

[18] Marocco P, Ferrero D, Lanzini A, Santarelli M. Optimal design of stand-alone solutions based on RES+ hydrogen storage feeding off-grid communities. Energy Conversion and Management. 2021;238:114147. https://doi.org/10.1016/j.enconman.2021.114147.

[19] Gravelsins A, Pakere I, Tukulis A, Blumberga D. Solar power in district heating. P2H flexibility concept. Energy. 2019;181:1023-35. https://doi.org/10.1016/j.energy.2019.05.224.

[20] Sayegh MA, Jadwiszczak P, Axcell BP, Niemierka E, Bryś K, Jouhara H. Heat pump placement, connection and operational modes in European district heating. Energy and Buildings. 2018;166:122–44. https://doi.org/10.1016/j.enbuild.2018.02.006.

[21] Arpagaus C, Bless F, Uhlmann M, Schiffmann J, Bertsch SS. High temperature heat pumps: Market overview, state of the art, research status, refrigerants, and application potentials. Energy. 2018;152:985–1010. https://doi.org/10.1016/J.ENERGY.2018.03.166.

[22] Wu W, Shi W, Li X, Wang B. Air source absorption heat pump in district heating: Applicability analysis and improvement options. Energy Conversion and Management. 2015;96:197–207. https://doi.org/10.1016/j.enconman.2015.02.068.

[23] Sciacovelli A, Guelpa E, Verda V. Multi-scale modeling of the environmental impact and energy performance of open-loop groundwater heat pumps in urban areas. Applied Thermal Engineering. 2014;71. https://doi.org/10.1016/j.applthermaleng.2013.11.028.

[24] Hiawen S, Tingyu W, Xin J, Zhiyong R, Haiyang Y, Duanmu L. Energy Efficiency Enhancement Potential of the Heat Pump Unit in a Seawater Source Heat Pump District Heating System. Procedia Engineering. 2016;146:134–8. https://doi.org/10.1016/j.proeng.2016.06.363.

[25] De Pasquale AM, Giostri A, Romano MC, Chiesa P, Demeco T, Tani S. District heating by drinking water heat pump: Modelling and energy analysis of a case study in the city of Milan. Energy. 2017;118:246–63. https://doi.org/10.1016/j.energy.2016.12.014.
[26] Lund R, Persson U. Mapping of potential heat sources for heat pumps for district heating in Denmark. Energy. 2016;110:129–38. https://doi.org/10.1016/j.energy.2015.12.127.
[27] David A, Mathiesen BV, Averfalk H, Werner S, Lund H. Heat Roadmap Europe: Large-scale electric heat pumps in district heating systems. Energies. 2017;10:1–18. https://doi.org/10.3390/en10040578.
[28] Østergaard PA, Andersen AN. Economic feasibility of booster heat pumps in heat pump-based district heating systems. Energy. 2018;155:921–9. https://doi.org/10.1016/j.energy.2018.05.076.
[29] Barco-Burgos J, Bruno JC, Eicker U, Saldaña-Robles AL, Alcántar-Camarena V. Review on the integration of high-temperature heat pumps in district heating and cooling networks. Energy. 2022;239:122378. https://doi.org/10.1016/j.energy.2021.122378.
[30] Ommen T, Markussen WB, Elmegaard B. Heat pumps in combined heat and power systems. Energy. 2014;76:989–1000. https://doi.org/10.1016/j.energy.2014.09.016.
[31] Bach B, Werling J, Ommen T, Münster M, Morales JM, Elmegaard B. Integration of large-scale heat pumps in the district heating systems of Greater Copenhagen. Energy. 2016;107:321–34. https://doi.org/10.1016/j.energy.2016.04.029.
[32] Vandermeulen A, van der Heijde B, Helsen L. Controlling district heating and cooling networks to unlock flexibility: A review. Energy. 2018;151:103-15. https://doi.org/10.1016/j.energy.2018.03.034.
[33] Lauka D, Gusca J, Blumberga D. Heat pumps integration trends in district heating networks of the Baltic States. Procedia Computer Science. 2015;52:835-42. https://doi.org/10.1016/j.procs.2015.05.140.
[34] Pensini A, Rasmussen CN, Kempton W. Economic analysis of using excess renewable electricity to displace heating fuels. Applied Energy. 2014;131:530-43. https://doi.org/10.1016/j.apenergy.2014.04.111.
[35] Kirkerud JG, Bolkesjø TF, Trømborg E. Power-to-heat as a flexibility measure for integration of renewable energy. Energy. 2017;128:776-84. https://doi.org/10.1016/j.energy.2017.03.153.
[36] Magni C, Quoilin S, Arteconi A. Evaluating the Potential Contribution of District Heating to the Flexibility of the Future Italian Power System. Energies. 2022;15(2):584. https://doi.org/10.3390/en15020584.
[37] Østergaard PA, Andersen AN. Variable taxes promoting district heating heat pump flexibility. Energy. 2021;221:119839. https://doi.org/10.1016/j.energy.2021.119839.
[38] Johannsen RM, Arberg E, Sorknæs P. Incentivising flexible power-to-heat operation in district heating by redesigning electricity grid tariffs. Smart Energy. 2021;2:100013. https://doi.org/10.1016/j.segy.2021.100013.
[39] Hennessy J, Li H, Wallin F, Thorin E. Flexibility in thermal grids: A review of short-term storage in district heating distribution networks. Energy Procedia. 2019;158:2430-4. https://doi.org/10.1016/j.egypro.2019.01.302.
[40] Quirosa G, Torres M, Chacartegui R. Analysis of the integration of photovoltaic excess into a 5th generation district heating and cooling system for network energy storage. Energy. 2022;239:122202. https://doi.org/10.1016/j.energy.2021.122202.
[41] Ayele GT, Mabrouk MT, Haurant P, Laumert B, Lacarrière B. Optimal heat and electric power flows in the presence of intermittent renewable source, heat storage and variable grid electricity tariff. Energy Conversion and Management. 2021;243:114430. https://doi.org/10.1016/j.enconman.2021.114430.
[42] Council of the European Union EP. Regulation (EU) 2019/943 of the European Parliament and of the Council of 5 June 2019 on the internal market for electricity. vol. 62. 2019. Available online: https://eur-lex.europa.eu/legal-content/EN/TXT/PDF/?uri=CELEX:32019R0943&from=EN.
[43] The SmartNet Consortium. TSO-DSO Coordination for Acquiring Ancillary Services From Distribution Grids. 2019. Availabe online: http://smartnet-project.eu/wp-content/uploads/2019/05/SmartNet-Booktlet.pdf.
[44] Città di Torino. Estensione rete di teleriscaldamento. Available online: https://www.torinovivibile.it/aree-tematiche/estensione-rete-di-teleriscaldamento/#.
[45] Mazza A, Chicco G. Losses Allocated to the Nodes of a Radial Distribution System with Distributed Energy Resources – A Simple and Effective Indicator. 2019 Int. Conf. Smart Energy Syst. Technol., Porto, Portugal: IEEE; 2019. https://doi.org/10.1109/SEST.2019.8849127.
[46] Badami M, Fambri G, Martino M, Papanikolaou A. ICT optimization tool for RES integration in combined energy networks. In INTELEC 2018 International Telecommunications Energy Conference, IEEE, Turin Oct 7th-11th 2018, Proceedings 2019. https://doi.org/10.1109/INTLEC.2018.8612376.
[47] Shirmohammadi D, Hong HW, Semlyen A, Luo GX. A compensation-based power flow method for weakly meshed distribution and transmission networks. IEEE Transactions on power systems. 1988;3(2):753-62. https://ieeexplore.ieee.org/document/192932.
[48] Badami M, Bompard E, Diaz-Londono C, Fambri G, Mazza A, Verda V. Deliverable D3.6 PLANET simulation model generator and integration to the distribution grid simulation suite. PLANET 2020. Available online: https://www.h2020-planet.eu/deliverables.
[49] Guelpa E, Sciacovelli A, Verda V. Thermo-fluid dynamic model of large district heating networks for the analysis of primary energy savings. Energy 2019;184:34–44. https://doi.org/10.1016/j.energy.2017.07.177.
[50] Guelpa E. Impact of thermal masses on the peak load in district heating systems. Energy. 2021;214:118849. https://doi.org/10.1016/j.energy.2020.118849.
[51] Pieper H, Ommen T, Buhler F, Lava Paaske B, Elmegaard B, Brix Markussen W. Allocation of investment costs for

large-scale heat pumps supplying district heating. Energy Procedia 2018;147:358–67. https://doi.org/10.1016/j.egypro.2018.07.104.

[52] Danish Energy Agency. Technology Data for Industrial Process Heat. 2020. Available online at: https://ens.dk/en/our-services/projections-and-models/technology-data/technology-data-industrial-process-heat

[53] Regulation (EU) 2019/943 of the European Parliament and of the Council of 5 June 2019 on the internal market for electricity. Official Journal of the European Union. Available online at: https://eur-lex.europa.eu/legal-content/EN/TXT/?uri=CELEX%3A32019R0943.

[54] Badami M, Mazza A, Estebsari A, Fambri A, Damousis Y, Terzi S, Ioannidis D, Sideris D, Tsadaris N, Katranas G, Papanikolaou A, Schröder A, Kahlen C, Berlioz S, McDowgall C. Deliverable D1.3 Definition of requirements and specifications for communication & grid interfaces. PLANET 2018. Available online: https://www.h2020-planet.eu/deliverables.